Journal of Pharmaceutical Research International

32(29): 18-30, 2020; Article no.JPRI.62165
ISSN: 2456-9119
(Past name: British Journal of Pharmaceutical Research, Past ISSN: 2231-2919, NLM ID: 101631759)

Computational Exploration of Potential Polo-Like Kinase 1 Inhibitors as New Chemotherapeutic Agents

Mubarak A. Alamri[1*] and Ahmed D. Alafnan[2]

[1]Department of Pharmaceutical Chemistry, College of Pharmacy, Prince Sattam Bin Abdulaziz University, P.O.Box 173, Al-Kharj 11942, Saudi Arabia.
[2]Department of Pharmacology and Toxicology, College of Pharmacy, University of Hail, Hail, Saudi Arabia.

Authors' contributions

This work was carried out in collaboration between both authors. Author MAA was involved in designing of experimental scheme, pharmacophore and docking-based virtual screening and prediction of ligands efficiency parameters and inhibitory constants. Author ADA was involved in molecular docking and molecular dynamics simulations studies. Both of the authors equally contributed in interpreting the results. Both authors read and approved the final manuscript.

Article Information

DOI: 10.9734/JPRI/2020/v32i2930880
Editor(s):
(1) Dr. Wenbin Zeng, Xiangya School of Pharmaceutical Sciences, Central South University, China.
Reviewers:
(1) Marwan M. Merkhan, University of Mosul, Iraq.
(2) Siddhartha Pati, University Malaysia Terengganu, Malaysia.
Complete Peer review History: http://www.sdiarticle4.com/review-history/62165

Original Research Article

Received 15 August 2020
Accepted 19 October 2020
Published 18 November 2020

ABSTRACT

Background and Objective: Polo like kinase-1 (PLK-1) enzyme belongs to serine/threonine protein kinase family that is regarded as a principle mitotic controller of G2-M phase transition. The antimitotic therapies are a cornerstone for the treatment of metastatic as well as benign cancer. Therefore, PLK-1 has recently gained much interest in the field of targeting it by novel and effective inhibitors.
Materials and Methods: The present study described the used of pharmacophore modelling based on the potent and selective clinical agent, Volasertib and followed by hybrid selection of a kinase inhibitors databank of 4800 diverse compounds by pharmacophore- and docking-based virtual screening.
Results: The retrieved hits were filtered on the bases of their pharmacophore-fit scores, docking

**Corresponding author: E-mail: m.alamri@psau.edu.sa;*

binding affinity scores, ADME-T profiles as well as ligand quality assessments. Among the five hit compounds that fulfil the criterion, three compounds, Z1991791422, Z56115729 and Z1991791176 were selected for binding dynamic analyses by molecular dynamic simulation. The Z1991791422 and Z56115729 compounds illustrated stable binding behaviours at the proposed binding site. **Conclusion:** Thus, these compounds might emerge as potent inhibitors of PLK1 and could be applied as seeds for designing better PLK1 inhibitors in near future.

Keywords: Autodock Vina; ligandscout; polo like kinase-1; pharmacophore; virtual screening; molecular simulation.

1. INTRODUCTION

Cancer remains a serious threat towards human health and has drawn grave scientific concern with the aim of developing a successful therapy to tackle it. For several decades, targeting the cell cycle processes, a hallmark of cancer, is a cornerstone therapeutic. Despite the efficacy of currently used clinical anti-microtubule agents like vinca alkaloid and taxanes, their severe dose-dependent toxicity has been a major therapeutic concern. The polo-like kinase-1 (Plk-1) belongs to serine/threonine protein kinase family, is a crucial mitotic regulator in transition of G2-phase of cell cycle to M-phase [1,2]. In addition to cell cycle, PLK-1 has been found to be associated with regulation of other cellular events such as DNA replication, metabolic pathways and NudC phosphyration mediated cytokinesis [1,3-7]. The structural basis of PLK-1 protein comprises of three domains, a typical kinase domain (KD) at *N*-terminal, an interdomain linker (IDL) and non-catalytic polo-box domain (PBD) at a *C*-terminal that is unique to PLK family. The PBD and KD have been found to be reciprocally inhibited, however, the clear mechanism is still unknown [8]. Among five PLK family structural homologs (i.e. PLK-1, -2, -3, -4 and -5), PLK-1 overexpression has been shown in variety of human cancers, for example, lung, prostate, intestinal, head-neck, breast, pancreas, thyroid, ovary, liver and skin [2,9-11] and is considered to be an independent prognostic marker in cancer patients [9,10]. Moreover, reports suggest that PLK-1 overexpression relate to reduced patient survival in some tumours [9,10,12]. It has been reported that inhibiting PLK-1 hindered the growth of triple negative breast cancer (TNBC) and bladder carcinoma [13,14]. Various reports suggesting the PLK-1 as an oncogene has inspired the scientific community to discover peculiar PLK-1 inhibitors. In the recent past, several studies have published; reporting PLK1 inhibition by various compounds and drugs [15,16]. As most of kinases, the PKL-1 kinase possess two typical sites that can be targeted by small-molecule inhibitors, first is the 'ATP binding pocket' within the *N*-terminus kinase domain, and the other is the substrate binding grove; the PBD domain [11]. Designing kinase inhibitors via focussing on 'catalytic kinase domain' has become a successful strategy in the recent past. Several ATP-competitive small-molecules inhibitors focusing on PLK-1 'kinase domain' have also been developed, and even some of them have reached clinical trials as well, for instance, Volasertib, GSK461364A, BI 2536, NMS-P937, TKM- 080301 and HMN-214 [17]. Volasertib is dihydropteridinone derivatives (developed by Boehringer Ingelheim) and is regarded as the standard inhibitor among these molecules due its pronounced potency in preclinical and clinical settings. The present study is designed with the aim to discover novel PLK-1 kinase domain inhibitors keeping in the mind their specificity and potency. In order to achieve our objective, the pharmacophore modelling in combination with virtual screening of a kinase inhibitors chemical database of 4800 compounds using Ligandscout and Autodock Vina were performed followed by ADMET analyses and ligands quality assessment to obtained potential lead molecules. The final obtained hits were then characterized for their dynamic stability behaviour at the binding pocket using all atoms molecular dynamic simulation.

2. MATERIALS AND METHODS

2.1 Generation of Pharmacophore Models and Their Validation Using Ligand Scout

The structure-dependent pharmacophore modelling is primarily focus on utilizing the binding interactions of protein–ligand complexes to create a plausible hypothesis. This has become a significant approach due to increased deposition of X-ray crystal structures in Protein Data Bank (PDB). Furthermore, the protein structure data is suggested to be an imperative

basis to design structure-dependent pharmacophore and utilized for primary screening prior to docking studies [18,19]. Therefore, the crystal structure of PLK-1 (residues 1 - 335) interacting with Volasertib, a potent small-molecule inhibitor, (PDB ID: 3FC2) was acquired from RCSB-PDB with an X-ray resolution of 2.45 Å [20]. LigandScout software [21] was used to deduce and identify the key interaction chemical characteristics as well as space pattern amongst PLK-1 and Volasertib to build and analyse 3D pharmacophore model. The Volasertib interaction pattern with the key amino acid residues of the 'catalytic domain' of PKL-1 provided appropriate data to construct structure-dependent pharmacophore model. However, for the qualitative validation of generated model receiver operating characteristic analysis was applied in LigandScout software. To select the final pharmacophore model two kinds of dataset were constructed, test set which is composed of 37 known active compounds and decoy set, which contains 410 compounds with unknown activity against PKL-1 kinase.

2.2 Selection of Chemical Database

In silico virtual screening was done with focused-protein kinase inhibitor library containing ~4800 ligand molecules to identify lead molecules toward PLK-1 kinase. The database was downloaded in SDF format from (available online on https://enamine.net/hit-finding/focused-libraries/kinase-library/allosteric-kinase-library).

2.3 Pharmacophore-Based Virtual Screening

The representative pharmacophore model was applied as a search query for the virtual screening of 4800 ligand molecules using LigandScout virtual screening tool. Initially, SDF files of compounds were imported to Ligandscout and converted into IDB format. The compounds that fit at least three pharmacophore features were obtained and ranked on the basis of their fit scores.

2.4 Docking-Based Virtual Screening

Autodock vina in PyRx 0.8 was used to perform docking-based virtual screening of 156 candidate compounds that were selected from initial screening. The flexible screening was performed against the 'catalytic site' of PLK-1 kinase (PDB ID: 3FC2). OpenBable tool applied in PyRx was used to convert the compounds from SDF into PDBQT format and for energy minimization. Then, the compounds having better binding energy scores in comparison to the known ligand, Volasertib were considered for further study.

2.5 *In silico* ADME, Toxcicity and Drug Likeness Predictions

The adsorption, distribution, metabolism and excretion (ADME) parameters such as intestinal absorption, blood-brain-barrier penetration, solubility, bioavailability and cytochrome P450 inhibition were predicted for screened compounds using online freely accessible online tool Swiss ADME (http://www.swissadme.ch/) [22]. The same web server was used to calculate the drug-likeness properties including Lipinski's rule of five such as no. of hydrogen bond donor and acceptor, log P, molecular weight, rotatable bonds, heavy atoms and polar surface area. The levels of toxicity such as mutagenicity and carcinotoxity, were estimated using a freely available webserver ProTox-II (available online on: http://tox.charite.de/protox_II/) was used [23,24] and the compounds that were non-mutagenic and non-carcinogenic were chosen for further assessment.

2.6 Ligand Quality and Activity Assessments

The quantitative quality assessment as well as inhibitory constants of obtained compounds was determined based on the Autodock vina scores of interaction/binding energy. The ligand efficiency (LE) and predicted inhibitory constants (*pKi*) of compounds were calculated using the following equations [25-27].

$$\text{Predicted inhibitory constants } pKi = 10^{[\text{Docking score } (\Delta E) \div 1.366]} \quad (1)$$

$$\text{Ligand efficiency } (LE) = -\Delta E \div (\text{heavy atoms}) \text{ HA} \quad (2)$$

2.7 Molecular Docking Using Autodock Vina

Autodock vina software was used to evaluate the binding pattern and interaction mechanism of identified hit compounds. The monomer PKL-1 structure (PDB ID: 3FC2) in complex with Volasertib was retrieved from RCSB-PDB [28]. Preparation of protein by eliminating water molecules and introduction of polar hydrogen atoms was executed by Discovery Studio

Visualizer 4.5 (Accelrys, San Diego, CA, USA). The same program was utilized for the generation of protein and ligand PDB files. Autodock tools performed conversion of target protein and ligands into PDBQT format and gridbox preparation to target specifically at PLK1 active site. The gridbox dimension was kept as X= 20 Y = 30 Z=18 with center coordinates as x = 47.855 y = -7.832 z = 9.893. To validate the parameters, the established ligand, Volasertib was redocked at same active site of PLK-1 using Autodock Vina and the resulted complex superimposed the previously obtained poses. The docking analysis and fig production were carried out by using PyMOL Molecular Graphics System 1.3 and Discovery Studio 4.5.

2.8 Molecular Dynamics (MD) Simulations

GROMACS 2018.1 software [29] was used to perform MD) simulation of protein-ligand docked complex. The topology of the protein was generated using OPLS-AA/L [30] force field while the docked ligand topology files and parameters were generated by the Swissparam server available at (http://www.swissparam.ch/) [31]. The MD simulation was performed by applying a procedure reported by Alamri [32]. TIP3P [33] water molecule models were used to solvate the docked protein-ligand complex followed by neutralizing the system with the counter ions. Periodic boundary parameters were applied throughout MD simulation and LINear Constraint Solver (LINCS) algorithm [34] was used to constrain bond lengths. The particle mesh Ewald method was used for electrostatic calculations. Steepest descent algorithm was applied for energy minimization of the system with 1000 kJ mol-1 nm-1 tolerance value followed by NVT and NPT based equilibration for 100 ps. At the end, MD was executed for the system for 100 ns with trajectories created after every 2 femto-second and snapshots were saved every 2 pico-second [35]. Grimaces utility commands gmx rmsf, gmx gyrate and gmx rms were used to analyze root mean square fluctuations (RMSF), radius of gyration and root mean square deviation (RMSD), respectively.

3. RESULTS

In the present study, initially the first pharmacophore was established by the interaction between the protein PLK-1 and its known ligand, Volasertib. The binding mode of Volasertib and essential residues within the binding pocket are presented in Fig. 1.

The generated pharmacophore was composed of three hydrophobic groups, three hydrogen bond acceptors and one hydrogen bond donor. These pharmacophore features were resulted from the interaction of Volasertib with essential residues within the binding site such as Leu59, Ala80, Leu130, Cys133 and Phe183 (Fig. 2A). The geometric arrangement of the pharmacophore features is illustrated in Fig. 2B.

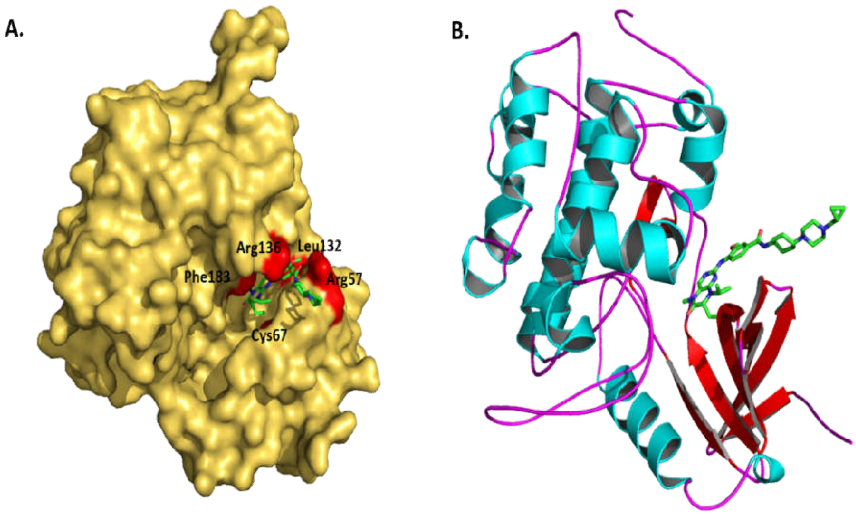

Fig. 1. PKL1 (PDB: 3FC2) X-ray crystal structure. (A) Molecular surface representation of PLK1 in complex with Volasertib (green). The essential binding residues were shown in red. (B) PLK1-Volasertib complex. PLK1 is presented in ribbon form with α helices (cyan) and β-sheets (red) and ligand volasertib were shown in green

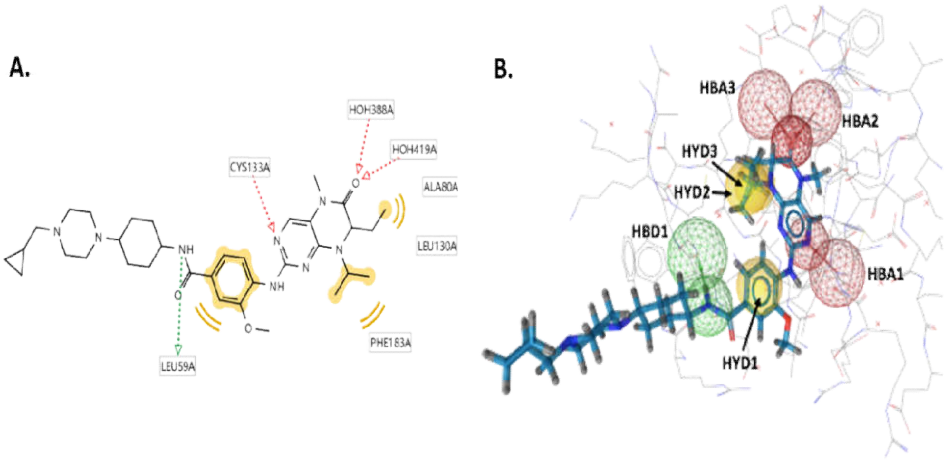

Fig. 2. (A) Interaction of Volasertib with PLK1 based on the X-ray structure (PDB: 3FC2). (B) Pharmacophore model generated on the basis of 'PLK1-Volasertib' interaction. Here, LigandScout represented colour coding for hydrogen bond donor (HBD) as green, hydrophobic groups (HYD) as yellow and hydrogen bond acceptor (HBA) as red

The final pharmacophore model with defined special arrangement is shown in Fig. 3A. This pharmacophore model was then tested to validate its sensitivity and ability to differentiate between active and inactive ligands by screening database composed of 410 decoy- and 37 active compounds. Fig. 3B showed the calculated value of receiver operating characteristics (ROC) plot, the area under the curve (AUC) and the enrichment factor (EF) at 1%, 5%, 10% and 100%. In this context, with an AUC value of 1, the initial enrichment factor was found to be 12.1 suggesting that obtained pharmacophore model was capable to rationally distinguish among decoy and active compounds. As a whole, in this performed virtual screening out of 447 compounds, 43 compounds were identified as hit compounds suggesting that the model demonstrated predilection towards active compounds with an AUC value of 0.94 and EF of 9.3.

The validated pharmacophore model was employed for screening focused-kinase inhibitors database having diverse ~ 4800 small-molecules. This exercise led to the identification of 156 compounds that could meet the pharmacophore-based virtual screening criteria. The pharmacophore fit score was used to rank the initial hits. Moreover, the selected compounds were further filtered on the basis of free binding energy score by docking-based virtual screening performed via Autodock vina in PyRx. Later on, 81 compounds were identified with high binding energy scores in comparison to the docked co-crystalized ligand, Volasertib that was used as a control.

Further, ADME profiling was performed by using SWISS-ADME web server and various toxicological endpoints (such as mutagenicity, oral toxicity and carcinogenicity) were measured using a web tool, ProTox-II. The compounds must be non-mutagenic and non-carcinogenic to be selected as a hit compound. In the end, only five hit compounds (Fig. 4) were yielded.

The docking scores (in kcal/mol) of the final hit compounds namely, Z169878688, Z1991791422, Z300646934, Z56115729, Z1991791176 were -8.0, -10.0, -7.1, -8.6 and -10.1, respectively. The molecular properties and ADMET profile is presented in Tables 1 and 2, respectively.

For further insight into the bioactivity and binding interaction of the identified hit compounds, the inhibitory constant based on Autodock vina binding energy score as well as the ligand efficiency which measures the binding energy of a compound relative to its size were calculated [36]. As shown in Table 3, the inhibitory constants of these compounds were predicted to be in a low micromolar concentration range. Z1991791176 was the most active one, then Z1991791422, Z56115729, Z169878688 and Z300646934 with predicted *Ki* values of 0.04, 0.05, 0.51, 1.39 and 6.34 µM, respectively. In term of the ligand efficiency (LE), hit compounds Z1991791422, Z56115729 and Z1991791176 passed the standard range limit indicating that

these hit compounds could serve as promising lead compounds Table 3.

Afterward, the filtered five hit compounds were subjected to molecular docking within the 'catalytic site' of PLK-1 using Autodock Vina. The binding pocket was defined and validated on the basis of interaction between PLK-1 (PDB: 3FC2) and Volasertib (Fig. 1). The docking validation was carried out by re-docking the Volasertib into the active site to validate the docking protocol successfully. Interestingly, the best docked posed of Volasertib was overlapped with the co-crystalized one with RMSD = 0.794 Å demonstrating the validity of the docking protocol (Fig. 5A). The 3D molecular interaction diagram of all the five hit compounds is shown in the Fig. 5B-F. The crucial common amino acid residues involved in all the five hit compounds were found to be Arg136, Phe183, Leu132, Arg57 and Cys67.

For further analysis, the hits compounds were mapped onto the pharmacophore model (Fig. 6). The results suggested that Z1991791422 and Z56115729 mapped on three hydrophobic, one hydrogen bond acceptor and donor (Fig. 6B and 6D), whereas Z1991791176 mapped one hydrophobic, one hydrogen bond acceptor and donor (Fig. 6E).

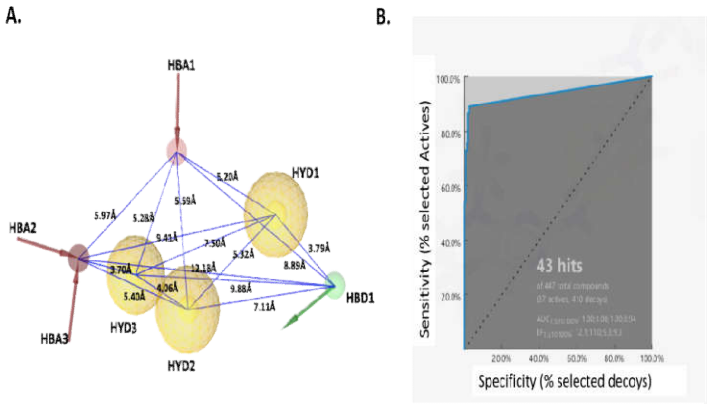

Fig. 3. Pharmacophore model generation and validation. (A) Final pharmacophore mode with geometrical distances. LigandScout presented pharmacophore features by colour codes in which green, red and yellow spheres indict hydrogen bond donor (HBD), hydrogen bond acceptor (HBA) and hydrophobic (HYD), respectively. (B) The receiver operating characteristics (ROC) validation curve of the final pharmacophore model

Table 1. Hit compounds molecular properties

Molecular property	Z169878688	Z1991791422	Z300646934	Z56115729	Z1991791176
Formula	**C20H22N2O5**	**C18H14N2O4S**	**C16H18N2O6S2**	**C14H11N3O5S**	**C18H14N2O5**
Mass	370	354	398	333	338
ClogP	3	2.6	1.8	1.4	1.8
HBA	4	4	5	4	4
HBD	3	2	3	4	2
Rotatable bounds	7	2	7	4	2
Polar Surface Area (PSA) /Å^2)	105	112	146	141	96
Lipinski's Rule of five violations	0	0	0	0	0
Refractivity	102	100	96	83	95
Heavy atoms (HA)	27	25	26	23	25

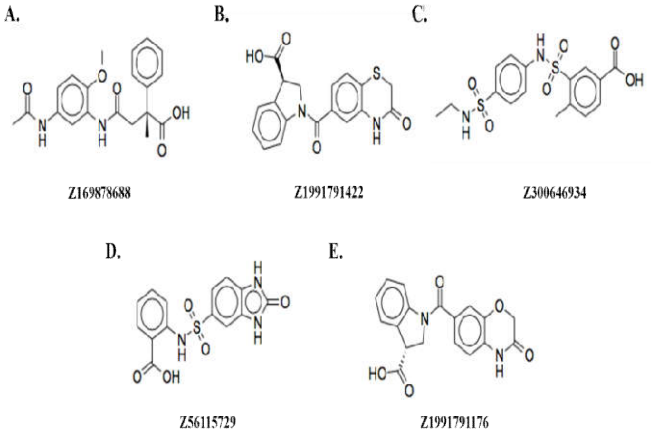

Fig. 4. Hit compounds chemical structures

Table 2. Hit compounds ADMET properties

Parameter	Z169878688	Z1991791422	Z300646934	Z56115729	Z1991791176
Absorption & Distribution					
BBB+	-1.16	-0.28	-1.14	-1	-0.37
HIA	56.7	96.1	58	65.2	72.8
Aqueous solubility (LogS)	-3.84	-3.94	-3.26	-2.89	-3.88
Bioavailability Score	0.56	0.56	0.56	0.55	0.56
Metabolism					
CYP Inhibitory Promiscuity	No	No	No	No	No
Toxicity					
AMES Toxicity	No	No	No	No	No
Carcinogenicity	No	No	No	No	No

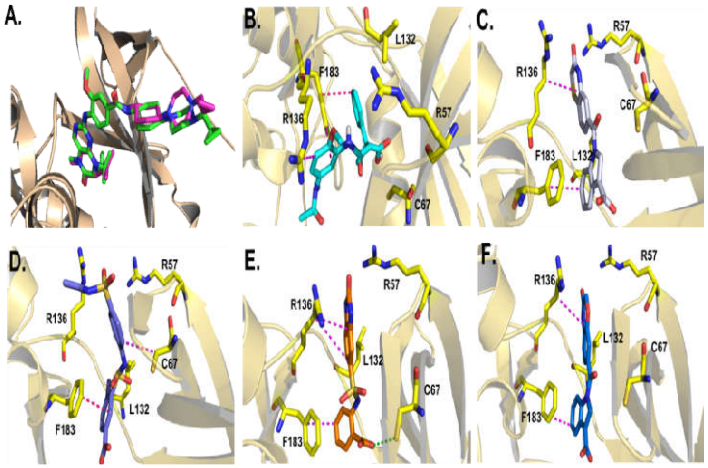

Fig. 5. Binding modes of candidate compounds to PLK1. (A) Best docked conformation of Volasertib (green) overlapped with co-crystal ligand (pink). (B) Molecular interactions of Z169878688 with the amino acid residues of PLK1 (C) Molecular interactions of Z1991791422, with the amino acid residues of PLK1 (D) Molecular interactions of Z300646934 PLK1 (E) The molecular interactions of Z56115729 with the amino residues in PLK1 (F) The molecular interactions of Z1991791176 with the amino residues in PLK1

Based on these results, we have selected compound Z1991791422, Z56115729 and Z1991791176 for molecular dynamics (MD) simulation studies. MD simulations for PLK-1 kinase complex with the three hits, Z1991791422, Z56115729 and Z1991791176 were performed for 20 ns to examine the binding stabilities. MD results were examined for the root-mean-squared deviations (RMSD), root-mean-squared fluctuations (RMSF) values and the radius of gyration (Rg) to assess the protein backbone stability. The results revealed that after ~ 2 ns with RMSD of about ~ 0.2 Å a converged and equilibrated state was achieved for all complexes. As shown in Fig. 7, Z1991791422 and Z56115729 complexes showed similar RMSD pattern with an averaged RMSD values of 0.16 ± 0.20 Å and 0.17 ± 0.24 Å, respectively. However, the RMSD profile of the Z1991791176 complex showed more oscillation between 13 and 16 ns and then returned back to a stable fluctuation pattern with average RMSD value of 0.17 ± 0.27 Å. The latter indicating that this ligand may adapt a new conformation at the binding site. To investigate the flexibility of protein residues during the MD simulation, RMSF of individual PLK-1 kinase residues were calculated. The RMSF values are shown in Fig. 8, suggested low backbone fluctuations with all systems indicating stable hits binding.

Similarly, the radius of gyration (Rg) which measures the compactness of protein showed stabile behaviour in the protein with average values of 2.0 ±0.011, 2.0± 0.011 and 1.99 ±0.012 nm in complex with Z1991791422,

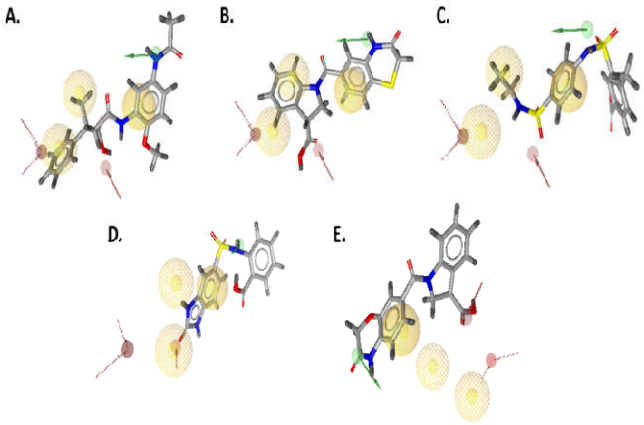

Fig. 6. Fit of the (A) Z169878688 (B) Z1991791422 (C) Z300646934 (D) Z56115729 (E) Z1991791176 to the structure-based pharmacophore model. LigandScout represented hydrogen bond donor, hydrogen bond acceptor and hydrophobic as green, red and yellow spheres, respectively

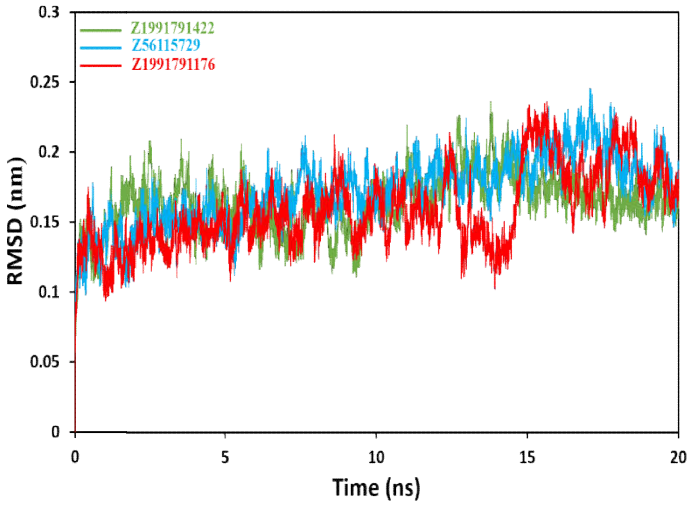

Fig. 7. RMSD values of the backbone atoms for PLK-1 kinase-inhibitors complexes

Table 3. Hit compounds molecular docking prediction against PLK1 via AutoDock Vina

Parameters	Z169878688	Z1991791422	Z300646934	Z56115729	Z1991791176
Docking score (kcal/mol)	-8	-10	-7.1	-8.6	-10.1
K_i (μM)	1.39	0.05	6.34	0.51	0.04
Ligand Efficiency (LE) / (kcal/mol/heavy atom)	0.3	0.4	0.27	0.37	0.4

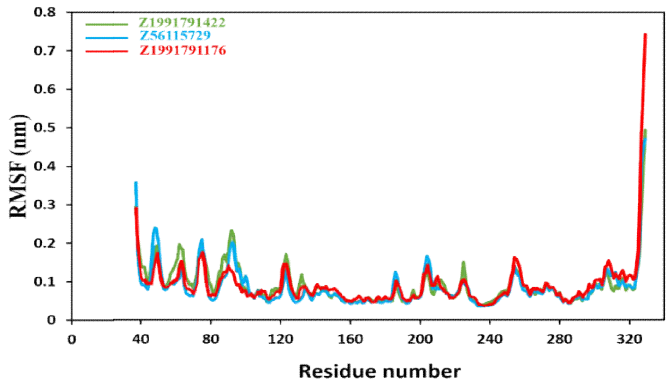

Fig. 8. RMSF values of each PLK-1 kinase residue

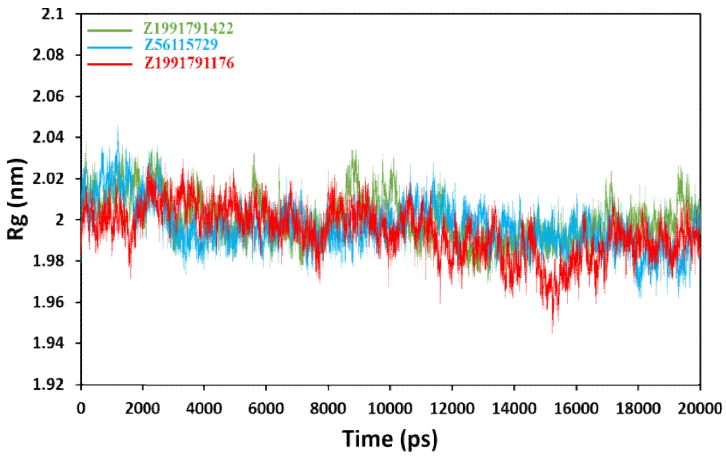

Fig. 9. Radius of gyration graph of PLK-1 kinase-inhibitors complexes

Z56115729 and Z1991791176, respectively (Fig. 9). In constant with RMSD results, Z1991791176 showed more fluctuation between 13000-16000 ps in comparison to other two ligands. Collectively, the MD analyses were in consistent with the docking results that these selected hits may bind with stable conformations to the active site of PLK-1 kinase and serve as potential lead compounds to inhibit its kinase activity.

4. DISCUSSION

The major reason of intricacy in cancer is involvement of several different pathophysiological features [37]. On the other hand, cancer prevalence has increased at a very sharp rate in the past few years that make it as one of the main reason of death globally [37,38]. Unfortunately, the currently available chemotherapeutic agents do not have the ability to target specifically to the cancer cells that might lead to toxicity issues; moreover, the cancer cells have developed resistance to these agents [39]. In addition, if you target one cancer pathway, alternate pathway would help cancer cell to survive in adverse conditions [40]. Hence, the paradigm has been shifted to find novel targets that are highly specific to cancer cells. One such cancer specific target is PLK1 and increased PLK1 expression has been found in different type

of cancer cells [2,9,10]. Importantly, it has been observed that PLK1 inhibition could hinder the growth of different cancer cells [13,14]. Thus, exploring novel PLK1 inhibitors have been the prime focus of the present study.

In the present study, Volasertib (a known PLK1 inhibitor) was used to establish the first pharmacophore. Later on, all the pharmacophore features including presence of hydrophobic regions, hydrogen bond donor and acceptor were revealed around the binding site of PLK-1 with geometric arrangement. These results were in agreement with reports of Shakil and Abuzinadah [24] and Sakkiah et al [41]. A hybrid virtual screening of a focused kinase library of 4800 molecules was performed against the obtained pharmacophore model of PLK-1 interacting with a known ligand, Volasertib. Overall, 156 candidate compounds were yielded from the virtual screening with reliable pharmacophore features and subjected to further study. Ranking of acquired molecules were based on their binding score which was followed by docking based virtual screening of those compounds against the active site of PLK-1 using Autodock Vina in PyRx program. Thus, out of 156 candidates, only 81 compounds were filtered with appropriate free energy binding score.

Consequently, ADMET (Absorption, Distribution, Metabolism, Elimination and Toxicity) properties profiling were performed which primarily eliminates weak drug candidates and provide necessary figs to screen the potential drug candidates. ADMET analysis was achieved by Swiss ADME server based on Lipinski's rule of five which includes:

(i) Molecular weight <500 Kda,
(ii) High lipophilicity,
(iii) HBD <5,
(iv) HBA <10, and,
(v) Molar refractivity 40-130.

At last, five hit compounds were filtered out of all the compounds based on their results. Moreover, these five hit compounds were subjected to molecular docking within the binding site of PLK-1 using Autodock Vina. Autodock Vina uses Monte-Carlo algorithm via applying gradient optimisation methods to provide more flexibility during docking. In fact, it is considered as a most appropriate tool for extensive screening [28]. More negative vina score is in a way linked to free binding energy ΔG that correlates with better binding of compounds with the target protein. In addition, it is a fact that weaker binding would eventually have fast dissociation rate [42]. In our study, hit compound Z1991791422, Z56115729 and Z1991791176 showed best binding results with the active site of PLK-1. The crucial common amino acid residues involved in all the five hit compounds were found to be Arg136, Phe183, Leu132, Arg57 and Cys67. It has been observed by Lu et al. [43] that interaction of compound (73) with Phe183 amino acid residue of PLK1 has shown important impact on entire compound conformational equilibrium. In another study, Arg136 and Phe183 were found to be important amino acid residues of PLK1 during binding of different anticancer drugs [16]. Furthermore, Shakil et al. [2] also observed the involvement of Cys67, Arg136 and Phe183 amino acid residues in PLK1-Volasertib interaction. Based on docking score we got some promising PLK1 inhibitors in our study.

Furthermore, molecular dynamics simulations studies were performed for best compounds i.e., hit compound Z1991791422, Z56115729 and Z1991791176. MD simulations are efficient in analysing the protein-ligand complex trajectory throughout the dynamics process to validate the docking stability in the entire process. RMSD, RMSF and Rg results showed that the protein complex with Z1991791422 and Z56115729 were more stable than Z1991791176. It is noteworthy to mention that MD simulations analyses corroborate our results of docking analysis. However, validation of obtained predicted results by further analysis is required to actually establish them as potent PLK1 inhibitors. Nevertheless, we could safely state that our findings on PLK1 inhibitors would provide some preliminary alternate options to the researchers trying hard to develop new anti-cancer therapy regime.

5. CONCLUSION

In the current study, we reported five novel orthosteric inhibitors of PLK-1 using Ligandscout based pharmacophore modelling, virtual docking screening and ADMET study. The structure-based pharmacophore model was generated by co-crystal complex of PLK-1 and its known ligand, Volasertib which consisted of hydrophobic bonds, hydrogen bond acceptors and hydrogen bond donors. Next, pharmacophore based virtual screening via ligandscout was accomplished by using an allosteric kinase library having 4800 compounds which leads to 156 candidate compounds. Further, docking based virtual

screening by Autodock Vina in PyRx yielded 81 candidate compounds. Finally, out of those 81 compounds only five compounds satisfied the ADMET criterion and Lipinski's rule of five and those ligands were called as hit compound. In conclusion, the expanding knowledge of the significance of PLK-1 over-expression in cancer cell cycle regulation and metabolism has necessitated the need of more effective potent PLK-1 inhibitors and indeed encouraged this *in-silico* study. We focussed the previously reported binding site on the PLK-1 which was effectively inhibited by Volasertib. The compounds obtained, especially Z1991791422, Z56115729 and Z1991791176, were found to be promising orthosteric ligands and may present themselves as potent inhibitors of PLK-1.

DISCLAIMER

The products used for this research are commonly and predominantly use products in our area of research and country. There is absolutely no conflict of interest between the authors and producers of the products because we do not intend to use these products as an avenue for any litigation but for the advancement of knowledge. Also, the research was not funded by the producing company rather it was funded by personal efforts of the authors.

CONSENT

It is not applicable.

ETHICAL APPROVAL

It is not applicable.

ACKNOWLEDGEMENTS

Mubarak A. Alamri would like to thank Prince Sattam Bin Abdulaziz University, Al Kharj, Saudi Arabia for providing necessary facilities to carry out this research. Ahmed D. Alafnan would like to thank University of Hail for providing computing facilities.

COMPETING INTERESTS

Authors have declared that no competing interests exist.

REFERENCES

1. Ma X, Wang L, Huang D, Li Y, Yang D, Li T, Li F, Sun L, Wei H, He K, Yu F, Zhao D, Hu L, Xing S, Liu Z, Li K, Guo J, Yang Z, Pan X, Li A, Shi Y, Wang J, Gao P, Zhang H. Polo-like kinase 1 coordinates biosynthesis during cell cycle progression by directly activating pentose phosphate pathway. Nat. Commun. 2017;8(1):1506.
2. Shakil S, Baig MH, Tabrez S, Rizvi SMD, Zaidi SK, Ashraf GM, Ansari SA, Khan AAP, Al-Qahtani MH, Abuzenadah AM, Chaudhary AG. Molecular and enzoinformatics perspectives of targeting polo-like kinase 1 in cancer therapy. Sem. Cancer. Biol. 2019;56:47-55.
3. Weerdt BCVD, Medema RH. Polo-like kinases: A team in control of the division. Cell Cycle. 2006;5(8):853-64.
4. Goetz MP, Toi M, Campone M, Sohn J, Paluch-Shimon S, Huober J, Park IH, Trédan O, Chen SC, Manso L, Freedman OC, Garnica JG, Forrester T, Frenzel M, Barriga S, Smith IC, Bourayou N, Di Leo A. MONARCH 3: Abemaciclib as initial therapy for advanced breast cancer. J. Clin. Oncol. 2017;35(32):3638-3646.
5. Sumara I, Vorlaufer E, Stukenberg PT, Kelm O, Redemann N, Nigg EA, Peters JM. The dissociation of cohesin from chromosomes in prophase is regulated by Polo-like kinase. Molecul. cell. 2002;9(3): 515-525.
6. Roshak AK, Capper EA, Imburgia C, Fornwald J, Scott G, Marshall LA. The human polo-like kinase, PLK, regulates cdc2/cyclin B through phosphorylation and activation of the cdc25C phosphatase. Cell. Signalling. 2000;12(6):405-11.
7. Kotani S, Tugendreich S, Fujii M, Jorgensen PM, Watanabe N, Hoog C, Hieter P, Todokoro K. PKA and MPF-activated polo-like kinase regulate anaphase-promoting complex activity and mitosis progression. Mol. Cell. 1998;1(3): 371-80.
8. Xu J, Shen C, Wang T, Quan J. Structural basis for the inhibition of Polo-like kinase 1. Nat. Struct. Mol. Biol. 2013;20(9):1047-53.
9. Weichert W, Schmidt M, Jacob J, Gekeler V, Langrehr J, Neuhaus P, Bahra M, Denkert C, Dietel M, Kristiansen G. Overexpression of polo-like kinase 1 is a common and early event in pancreatic cancer. Pancreatol. 2005;5(2):259-65.
10. Weichert W, Kristiansen G, Winzer KJ, Schmidt M, Gekeler V, Noske A, Müller BM, Niesporek S, Dietel M, Denkert C. Pololike kinase isoforms in breast cancer: Expression patterns and prognostic

implications. Virchows. Arch. 2005;446: 442-50.
11. Abdelfatah S, Berg A, Böckers M, Efferth T. A selective inhibitor of the Polo-box domain of Polo-like kinase 1 identified by virtual screening. J. Adv. Res. 2019;16: 145-156.
12. Wolf G, Elez R, Doermer A, Holtrich U, Ackermann H, Stutte HJ, Altmannsberger HM, RuÈbsamen-Waigmann H, Strebhardt K. Prognostic significance of polo-like kinase (PLK) expression in non-small cell lung cancer. Oncogene. 1997;14(5):543-49.
13. Seth S, Matsui Y, Fosnaugh K, Liu Y, Vaish N, Adami R, Harvie P, Johns R, Severson G, Brown T, Takagi A. RNAi-based therapeutics targeting survivin and plk1 for treatment of bladder cancer. Mol. Ther. 2011;19(5):928-35.
14. Hu K, Law JH, Fotovati A, Dunn SE. Small interfering RNA library screen identified polo-like kinase-1 (PLK1) as a potential therapeutic target for breast cancer that uniquely eliminates tumor-initiating cells. Breast Cancer Res. 2012;14(1):R22.
15. Rizvi SMD, Shakil S, Zeeshan M, Khan MS, Shaikh S, Biswas D, Ahmad A, Kamal MA. An enzoinformatics study targeting polo-like kinases-1 enzyme: Comparative assessment of anticancer potential of compounds isolated from leaves of *Ageratum houstonianum*. Pharmacog. Mag. 2014;10:S14-21.
16. Rizvi SMD, Alshammari AAA, Almawkaa WA, Ahmed ABF, Katamesh A, Alafnan A, Almutairi TJ, Alshammari RF. An oncoinformatics study to predict the inhibitory potential of recent FDA-approved anti-cancer drugs against human Polo-like kinase 1 enzyme: A step towards dual-target cancer medication. 3 Biotech. 2019;9(3):70.
17. Strebhardt K, Becker S, Matthess Y. Thoughts on the current assessment of Polo-like kinase inhibitor drug discovery. Expert. Opin. Drug. Dis. 2015;10(1):1-8.
18. Raab M, Pachl F, Krämer A, Kurunci-Csacsko E, Dötsch C, Knecht R, Becker S, Kuster B, Strebhardt K. Quantitative chemical proteomics reveals a Plk1 inhibitor-compromised cell death pathway in human cells. Cell. Res. 2014;24(9): 1141-45.
19. Alamri MA, Alamri MA. Pharmacophore and docking-based sequential virtual screening for the identification of novel Sigma 1 receptor ligands. Bioinformation. 2019;15(8):586-595.
20. Rudolph D, Steegmaier M, Hoffmann M, Grauert M, Baum A, Quant J, Haslinger C, Garin-Chesa P, Adolf GR. BI 6727, a Polo-like kinase inhibitor with improved pharmacokinetic profile and broad antitumor activity. Clin. Cancer Res. 2009;15(9):3094-102.
21. Wolber G, Langer T. LigandScout: 3-D Pharmacophores derived from protein-bound ligands and their use as virtual screening filters. J. Chem. Info. Model. 2005;45(1):160-69.
22. Daina A, Michielin O, Zoete V. SwissADME: A free web tool to evaluate pharmacokinetics, drug-likeness and medicinal chemistry friendliness of small molecules. Sci. Rep. 2017;7:42717.
23. Banerjee P, Eckert AO, Schrey AK, Preissner R. ProTox-II: A webserver for the prediction of toxicity of chemicals. Nucleic. Acids. Res. 2018;46(W1):W257-W263.
24. Shakil S, Abuzinadah MF. Putative anti-cancer drug candidate targeting the 'PLK-1-Polo-Box Domain' by high throughput virtual screening: A computational drug design study. Crit. Rev. Eukaryot. Gene. Expr. 2019;29(3):251-61.
25. Onawole AT, Kolapo TU, Sulaiman KO, Adegoke RO. Structure based virtual screening of the Ebola virus trimeric glycoprotein using consensus scoring. Comput. Biol. Chem. 2018;72:170-80.
26. Edwards MP, Price DA. Role of physicochemical properties and ligand lipophilicity efficiency in addressing drug safety risks. Annu. Rep. Med. Chem. 2010;45:380-391.
27. Murray CW, Erlanson DA, Hopkins AL, Keserü GM, Leeson PD, Rees DC, Reynolds CH, Richmond NJ. Validity of ligand efficiency metrics. ACS Med. Chem. Lett. 2014;5(6):616-8.
28. Trott O, Olson AJ. AutoDock Vina: Improving the speed and accuracy of docking with a new scoring function, efficient optimization and multithreading. J. Comp. Chem. 2010;31(2):455-61.
29. Hess B, Kutzner C, Van Der Spoel D, Lindahl E. GROMACS 4: Algorithms for highly efficient, Load-balanced, and scalable molecular simulation. J. Chem. Theory. Comput. 2008;4(3):435-47.
30. Kaminski GA, Friesner RA, Tirado-Rives J, Jorgense WL. Evaluation and

reparameterization of the opls-aa force field for proteins via comparison with accurate quantum chemical calculations on peptides. J. Phys. Chem. B. 2001;105: 6474−87.
31. Zoete V, Cuendet MA, Grosdidier A, Michielin O. SwissParam: A fast force field generation tool for small organic molecules. J. Comput. Chem. 2011;32(11): 2359-68.
32. Alamri MA. Pharmacoinformatics and molecular dynamic simulation studies to identify potential small-molecule inhibitors of WNK-SPAK/OSR1 signaling that mimic the RFQV motifs of WNK kinases. Arab. J. Chem. 2020;13(4):5107-17.
33. Jorgensen WL, Chandrasekhar J, Madura JD, Impey RW, Klein ML. Comparison of simple potential functions for simulating liquid water. J. Chem. Phys. 1983;79(2): 926-35.
34. Hess B, Bekker H, Berendsen HJ, Fraaije JG. LINCS: A linear constraint solver for molecular simulations. J. Comput. Chem. 1997;18(12):1463-72.
35. Tripathi S, Kumar A, Kumar BS, Negi AS, Sharma A. Structural investigations into the binding mode of novel neolignans Cmp10 and Cmp19 microtubule stabilizers by *in silico* molecular docking, molecular dynamics and binding free energy calculations. J. Biomol. Struct. Dyn. 2016;34(6):1232-40.
36. Kenny PW. The nature of ligand efficiency. J. Cheminformatics. 2019;11(1):8.
37. Padma VV. An overview of targeted cancer therapy. Biomed. 2015;5(4):19.
38. Jemal A, Bray F, Center MM, Ferlay J, Ward E, Forman D. Global cancer statistics. CA Cancer J. Clin. 2011;61:69-90.
39. Xu G, McLeod HL. Strategies for enzyme/prodrug cancer therapy. Clin. Cancer. Res. 2001;7:3314-24.
40. Xie L, Bourne PE. Developing multi-target therapeutics to fine-tune the evolutionary dynamics of the cancer ecosystem. Front. Pharmacol. 2015;6:209.
41. Sakkiah S, Senese S, Yang Q, Lee KW, Torres JZ. Dynamic and multi-pharmacophore modeling for designing polo-box domain inhibitors. PLoS. One. 2014;9(7):e101405.
42. Copeland RA. Conformational adaptation in drug-target interactions and residence time. Future. Med. Chem. 2011;3(12): 1491-501.
43. Lu S, Liu HC, Chen YD, Yuan HL, Sun SL, Gao YP, Yang P, Zhang L, Lu T. Combined pharmacophore modeling docking and 3D-QSAR studies of PLK1 inhibitors. Int. J. Mol. Sci. 2011;12:8713-39.

Peer-review history:
The peer review history for this paper can be accessed here:
http://www.sdiarticle4.com/review-history/62165